Modeling of Back-Propagation Neural Network Based State-of-Charge Estimation for Lithium-Ion Batteries with Consideration of Capacity Attenuation

Shuzhi ZHANG, Xu GUO, Xiongwen ZHANG
MOE Key Laboratory of Thermo-Fluid Science and Engineering
Xi'an Jiaotong University, Shaanxi 710049, China
xwenz@mail.xjtu.edu.cn

***Abstract*—The state of charge of lithium-ion batteries reflects the power available in the battery. Precise SOC estimation is a challenging task for battery management system. In this paper, a novel hybrid method by fusion of back-propagation (BP) neural network and improved ampere-hour counting method is proposed for SOC estimation of lithium-ion battery, which considers the impact of battery capacity attenuation on SOC estimation during the process of charging and discharging. The predictive accuracy and effectiveness of model are validated by NASA lithium-ion battery dataset. Moreover, the adaptability and feasibility of this method are further demonstrated using dataset of accelerated life experiment. The validation results indicate that the proposed method can provide accurate SOC estimation in different capacity attenuation stage.**

***Index Terms*—attenuation measurement, backpropagation, battery management systems, lithium batteries, neural networks.**

I. INTRODUCTION

Batteries directly contribute to the advancement of technologies ranging from portable electronics to fuel efficient vehicles [1]. Due to the superior performance, such as light weights [2], high energy density, low self-discharge rate, no memory effect [3], long lifetime and so on [4], lithium-ion batteries stand out among rechargeable secondary batteries and are widely used in electric vehicles (EVs) as the main power source and energy storage unit. In order to enhance the performance of the lithium-ion battery, a battery management system (BMS) is required to provide protection and monitor the power battery in an all-around way [5]. For battery management, accurate estimations of state of charge (SOC) is crucial [6]. The United States Advanced Battery Consortium (USABC) defines SOC as the percentage of the remaining capacity in the rated capacity under the same conditions [7]. It is an indicator not only for predicting the remaining mileage of EVs but also for determining a safe management strategy to avoid battery over-charge and over-discharge [8-11]. The precise SOC value can characterize the battery usage and the degree of charging/discharging, thus providing a basis for the formulation of ideal battery charge/discharge strategy.

Project Supported by the National Key Research and Development Program of China (2016YFB0901900).

Batteries typically have nonlinear and time-varying characteristics [12]. In practical applications, it is very difficult to estimate SOC accurately because of imprecise initial SOC and heavy calculation. At present, a number of research methods have been put forward to estimate SOC, which can be mainly classified into three categories: (1) experiment-based methods; (2) model-based methods; and (3) data-driven methods. Each one has its own advantages and disadvantages in certain aspects [13].

(1) Experiment-based methods: experiment-based methods mainly include open circuit voltage method [14-17], internal resistance method and ampere-hour counting method. The open circuit voltage method is very similar to the internal resistance method. The two methods firstly measure the open circuit voltage or resistance and then estimate the SOC value according to the corresponding relationship between the open circuit voltage/resistance and SOC. These two methods are rarely applied in practice due to the long time spent in the experiment or the existence of interference factors in the experiment. Due to fast computation and easy implementation, ampere-hour counting method is most widely used under SOC estimation method in real term applications [18, 19]. The advantage of this method is that it is not necessary to study the working principle of the battery or establish a model. It only needs to integrate the inflow or outflow current in a certain period of time, and then calculate the SOC value at the current moment according to the initial SOC value. However, its disadvantages are also obvious: the estimation accuracy is excessively dependent on the accuracy of the initial SOC value, the precise sensors are required and the measurement error is also accumulated along SOC estimation [20]. In addition, the rated capacity of lithium-ion battery also decreases after a large number of charge/discharge cycles, which also brings certain errors to the estimation of SOC value.

(2) Model-based methods: typical battery models involve the electrochemical model [21], the electro-thermal model [22], the equivalent circuit model (ECM) [23] and the computational intelligence based model [24]. The ECMs are used to reproduce the battery dynamics with a variety of adaptive filters, such as extended Kalman filter (EKF) [25, 26] and its variants [27, 28], particle filter [29, 30], H-

Digital Object Identifier 10.4316/AECE.2019.03001

infinity observer [31] and sliding mode observer [32, 33]. Unfortunately, the model-based techniques are difficult to be applied in BMS due to large matrix operations [34].

(3) Data-based methods: with the development of artificial intelligence, data-based methods have been proposed in recent years, including BP neural network [35, 36], support vector machine [37], fuzzy logic principles [38] and so on. Malkhandi et al. [39] used the fuzzy logic to estimate SOC; Sheng et al. [40] proposed the fuzzy least square support vector machine to reduce the noise sensitive issue of common machine learning strategies; Hussein et al. [41] presented two BP neural networks for SOC estimation. Their model-free characteristics and flexibility make them suitable for nonlinear mapping approximations [42]. Since the battery is affected by various chemical factors, the value of SOC is variable. Such methods can automatically adjust internal parameters according to changes in the system, which is a class of ideal SOC estimation methods [43, 44]. However, the estimation accuracy strongly depends on the quality and quantity of the experimental data [45]. Hence, the accuracy of the neural network output is closely related to the accuracy of the original training data. Only when the training data is sufficiently accurate, the output of the neural network is of practical significance. Therefore, the premise of improving the output accuracy of BP neural network is to improve the accuracy of SOC training data.

In this study, ampere-hour counting method is improved on the attenuation of rated capacity in the charging and discharging cycle of the battery. Using the calculation results of this improved method, the BP neural network is trained and validated based on the lithium-ion battery dataset from NASA. Finally, the adaptability and feasibility of this fusion method are verified by dataset of accelerated life experiment.

The rest structure of this paper is arranged as follows: Section 2 introduces the novel method by fusion of BP neural network and improved ampere-hour counting method. Section 3 describe the establishment process of SOC estimation model in detail. Section 4 presents the training and validation results of model. And the key conclusions are summarized in Section 5.

II. METHODOLOGIES

Lithium-ion battery meets the requirements of charging and discharging cycles because its positive and negative active materials can reversibly intercalate or de-intercalate lithium ions. However, in actual use, the attenuation of battery capacity is inevitable. The causes of capacity attenuation in lithium-ion batteries include [46]: overcharge, growth of solid electrolyte interface film (SEI), decomposition of electrolyte, dissolution of active materials and phase transition.

The degree of capacity attenuation of lithium-ion batteries represents the degree of aging. As the number of charging and discharging cycles increases, the battery capacity gradually decreases, and the degree of aging increases. The accurate estimation of the battery capacity value can not only monitor the aging degree of the battery so as to timely replace the battery and ensure its reliability and safety, but also correct the SOC state of the battery and improve the accuracy of SOC estimation [47, 48]. Therefore, improving the estimation accuracy of battery capacity value is of great significance to the SOC estimation.

Ampere-hour counting method is one of the most commonly used SOC estimation methods, and its mathematical expression is:

$$\mathrm{SOC} = SOC_0 - \frac{1}{C_n}\int_0^t \eta I dt \tag{1}$$

Where SOC_0 is the initial value, C_n is the rated capacity of the battery, η is the Coulomb coefficient, and I is the charge and discharge current.

As mentioned above, the estimation accuracy of this method is not only related to the accuracy of the initial SOC value and current sensor, but also affected by the rated capacity of battery. Therefore, with the increase of charging and discharging cycles, the attenuation of the capacity is also a problem that must be considered when using the ampere-hour counting method. In order to solve the problem of SOC estimation error caused by battery capacity attenuation, the calculation formula of ampere-hour counting method has to be improved. A new variable called cycle number (N) is defined to consider the effect of capacity attenuation during the charging and discharging process. The improved ampere-hour counting formula is as follows:

$$\mathrm{SOC} = SOC_0 - \frac{1}{C_n(N)}\int_0^t \eta I dt \tag{2}$$

Here, $C_n(N)$ represents the rated capacity of the lithium-ion battery during the N^{th} charging and discharging cycle.

The specific operation method is as follows:

Step 1: charging and discharging a new type of lithium-ion battery under a certain temperature.

Step 2: Select a certain time step to measure and record the instantaneous voltage value, current value and surface temperature value of the battery, and measure the rated capacity of the battery at the end of each charging and discharging cycle, record the number of cycles and the corresponding rated capacity measurement value.

Step 3: Then the curve fitting is carried out for the number of cycles and their corresponding rated capacity, and the curve with the best fitting effect is finally selected to determine the relationship between rated capacity and the number of cycles of charging and discharging.

The integral term of the current with respect to time in the ampere-hour counting method is processed as follows: according to the measured data, a current-time scatter plot is made, and the mean square error and the determination coefficient of various types of fitting curves are also compared. Next, select the appropriate curve to fit the data points, record the fitting results and further calculate the integrated value of the current with respect to time.

The SOC of lithium-ion battery at the time of full charge is taken as the initial value of SOC. Then the integral value of $C_n(N)$ and current with respect to time is substituted into the formula of the improved ampere-hour counting method. Considering the capacity attenuation, the SOC in the discharging process of the battery can be calculated, which is used as the training data of BP neural network in the next step.

Back propagation (BP) neural network is a multi-layer feed-forward neural network trained according to the error back propagation algorithm [49]. It is the most widely used in various neural networks with the characteristics of signal forward transmission and error back-propagation. The structure of BP neural network consists of a three-layer model, including an input layer, hidden layer, and output layer. Theoretically, it has been proved that the three-layer neural network has the ability to simulate arbitrarily complex nonlinear mappings as long as the number of hidden layer nodes is sufficient. The BP neural network model [50] is shown in Fig. 1.

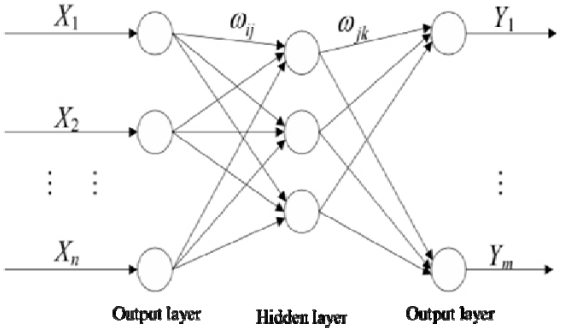

Figure 1. BP neural network topology diagram

The forward propagation of the signal is mainly divided into two stages: first, the variable X of the input layer, the connection weight ω_{ij} between the input layer and the hidden layer and the bias b_j of the hidden layer are calculated to obtain the output H of the hidden layer:

$$H_j = f\left(\sum_{i=1}^{n}\omega_{ij}x_i + b_j\right), j = 1,2,\ldots,l \quad (3)$$

l is the number of the hidden layer nodes and f is the activation function of the hidden layer.

Second, after calculating the output H of the hidden layer, the final output O of the neural network is output according to the connection weight ω_{jk} and the bias b_j between the hidden layer and the output layer:

$$O_k = f\left(\sum_{j=1}^{n}\omega_{jk}H_j + b_j\right), k = 1,2,\ldots,m \quad (4)$$

Where m is the number of nodes of the output layer.

The BP neural network error's back propagation is also divided into two stages: first, the prediction error e is calculated based on the final output O and the theoretical real value Y. There are a variety of calculation formulas for the prediction error e. Here is an example of the mean square error formula:

$$e_k = \frac{1}{2}\sum_{k=1}^{m}\left(Y_k - O_k\right)^2, k = 1,2,\ldots,m \quad (5)$$

According to the connection weight between each two layers, the error e_k is distributed and then propagated to each layer in the reverse direction. Then the partial derivative of the connection weight and the bias is obtained to make the adjustment proportional to the gradient descent of the error. Take the connection weight between hidden layer and output layer as an example:

$$\Delta\omega_{jk} = -\gamma\frac{\partial e_k}{\partial\omega_{jk}}, j = 1,2,\ldots,l; k = 1,2,\ldots,m \quad (6)$$

Where γ is learning rate, which represents the degree of adjustment of the connection weight and the bias, usually between 0-1.

After all the connection weight values and bias values in the network have been updated, the error function is calculated again. When the error function satisfies the set output requirements, the reverse error propagation stops, and all weight and bias values are saved. The BP neural network training is completed.

III. Model Description

In order to develop high-power lithium-ion batteries and solve the power problem of hybrid electric vehicles, NASA selected the 18650 lithium-ion battery as the research object and carried out accelerated life experiment on platform of lithium-ion battery, and obtained a series of NASA data. Based on this dataset, the BP neural network was constructed and trained.

The specific operating conditions of battery 5# are as follows: firstly, the battery is charged at a constant current (CC) of 1.5A until the voltage reaches 4.2V, then maintain the state of constant voltage (CV), and the charging process is completed when the current drops to 20mA. Correspondingly, the battery is discharges at a constant current (CC) of 2A until the voltage drops to 2.7V. Then the rated capacity of the battery is measured and the number of cycles of charge and discharge is recorded. The experiment stops when the measured value of the rated capacity attenuates to 70% of the nominal capacity.

Before training the BP neural network, the number of nodes of input layer, hidden layer and output layer should be determined first. For input layer, the number of nodes represents the number of eigenvalues. At present, the battery voltage, current and surface temperature are generally selected as the input eigenvalues in the model using BP neural network to predict the SOC. In order to consider the effect of capacity attenuation of lithium-ion battery, the number of charging and discharging cycles N was introduced in section 2. Therefore, voltage, current and surface temperature of battery, measurement time and number of cycles are selected as five input eigenvalues (nodes) of the neural network. Since the neural network output is SOC, the number of output layer nodes is 1.

There are several methods for determining the number of neurons in the hidden layer:

$$h = \sqrt{p+q} + a \quad (7)$$

$$h = \log_2 p \quad (8)$$

$$h = 2p + 1 \quad (9)$$

Where h, p, and q are the number of neurons in the hidden layer, the input layer, and the output layer, respectively, and a is a constant between 1 and 10. If the number of hidden layer nodes is too small, the analysis ability of the sample data is reduced. However, if the number of nodes is too large, the amount of calculation is increased, and the error function may not be minimized. The number of nodes in the hidden layer is changed

successively, the mean square error function is selected as the error function, and the normalized training data is used to train 500 iterations. The error values when the network training stopped are shown in Table 1. Therefore, the number of hidden layer nodes is selected as 12 because of its smallest error value. The final structure of BP neural network is three-layered as 5-12-1.

TABLE I. MEAN SQUARE ERROR VALUE AFTER 500 ITERATIONS FOR DIFFERENT NUMBER OF HIDDEN LAYER NODES

Number of nodes	Mean square error
8	1.984
9	7.189
10	1.353
11	0.325
12	0.0980
13	0.375

The activation function in the BP neural network is the core of the neural network. It transforms the output of each layer nonlinearly, and makes it capable of predicting the nonlinear relationship between input and output. The performance of neural network is affected by different activation functions. The commonly used activation functions are *sigmoid* function, *tanh* function and *ReLU* function. Fig. 2 (a) shows *sigmoid* function whose figure is differentiable throughout the interval. The *tanh* function is symmetric around the origin, which is shown in Fig. 2 (b). *Sigmoid* function and *tanh* function have the same disadvantage: when they tend to be larger or smaller values, the change of the whole function is relatively flat, that is, the gradient change is small, which will affect the learning efficiency of the network. In order to ensure the learning efficiency of neural network, *ReLU* function is often used as the activation function in practical work. The image of *ReLU* function is shown in Fig. 2 (c).

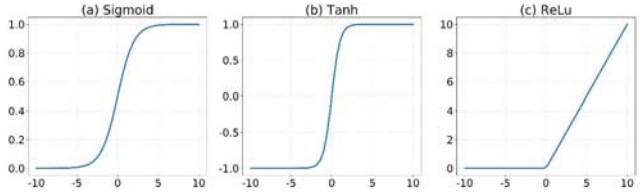

Figure 2. (a) Sigmoid activation function. (b) Tanh activation function. (c) Relu activation function.

In the BP neural network, an error function is usually defined when training the model with initial data. This error function value is minimized by algorithm such as gradient descent to improve the performance of the model. In this paper, average relative error function E is defined as the error function for SOC estimation:

$$E = \frac{1}{m}\sum_{k=1}^{m}\left|\left(Y_k - O_k\right)/Y_k\right|, k = 1,2,\ldots,m \qquad (10)$$

Where Y_k is the theoretical value, and O_k is the predicted value of the neural network.

According to the change of learning rate in BP neural network, the optimizer can be roughly divided into traditional and adaptive learning rate optimization algorithm. In traditional optimization algorithm, the learning rate is set to be constant or adjusted according to the number of iterations, so the training speed and accuracy of the model are often unsatisfactory. To overcome the drawbacks of traditional optimization algorithm, adaptive learning rate optimization algorithm is proposed: the learning rate is adjusted according to the gradient and the error value, which not only improves the training speed of the model, but also ensures the accuracy of the training results. In this study, the AdaDelta optimizer is selected to train the model, which has the ability to automatically adjust the learning rate according to the instant training results. In order to ensure the speed of the pre-mid-term training, the initial value of the learning rate was set to 0.9.

In addition, it is necessary to normalize the data before training the neural network, which can reduce the iterative steps of the optimizer to obtain the optimal solution for the error function and improve the accuracy of the neural network. In this study, the training set and validation set are normalized using the Z-score (standardization) method. This method generalizes all the data into a distribution with mean value of 0 and variance of 1 by linear transformation, so that the normalized data will not produce large deviation. For the normalization of the training set, the formula is as follows:

$$X_{\text{scale-train}} = \left(X_{\text{train}} - X_{\text{mean-train}}\right)/\sigma_{\text{train}} \qquad (11)$$

Where $X_{\text{scale-train}}$ is new training set after normalization, X_{train}, $X_{\text{mean-train}}$ and σ_{train} are every eigenvalue, the mean of the eigenvalue and the standard deviation of the eigenvalue in the original training set, respectively.

For the data of the validation set, the normalized formula is as follows:

$$X_{\text{scale\_test}} = \left(X_{\text{test}} - X_{\text{mean-train}}\right)/\sigma_{\text{train}} \qquad (12)$$

In the formula, $X_{\text{scale\_test}}$ is new validation set after normalization, X_{test}, $X_{\text{mean-train}}$ and σ_{train} are every eigenvalue, the mean of the eigenvalue and the standard deviation of the eigenvalue in the original validation set, respectively.

IV. RESULTS AND DISCUSSION

The curve fitting of rated capacity and number of cycles is shown in Fig. 3. By comparing coefficient of determination and the mean square deviation of various types of fitting curves, the cubic polynomial is finally selected as the type of the final fitted curve.

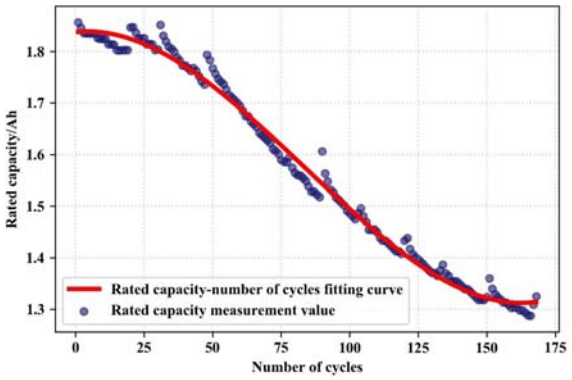

Figure 3. Rated capacity-number of cycles fitting curve based on NASA dataset.

And the fitting result is as follows:

$$C_n(N) = 1.83712 + 6.01435*10^{-4}*N - 6.69958*10^{-5}*N^2 + 2.6718*10^{-7*}N^3 \quad (13)$$

Based on the dataset of NASA lithium-ion battery, the battery voltage, current, surface temperature, measurement time and number of charging and discharging cycles of battery 5# are selected as the input eigenvalues, and the SOC calculated by the improved ampere-time counting method is selected as output of BP neural network. The neural network is trained after normalizing the data. Fig. 4 shows the variation of the average relative error of the BP neural network when the number of iterations is set to 1000. As we can see, the average relative errors are very high in the early stage of training. However, due to the large initial learning rate and high learning efficiency, the average relative errors decrease rapidly. When the iterations reach 500, the learning rate decreases, and the average relative errors change relatively slowly at this time. When the training process is completed, the average relative error reaches 39%.

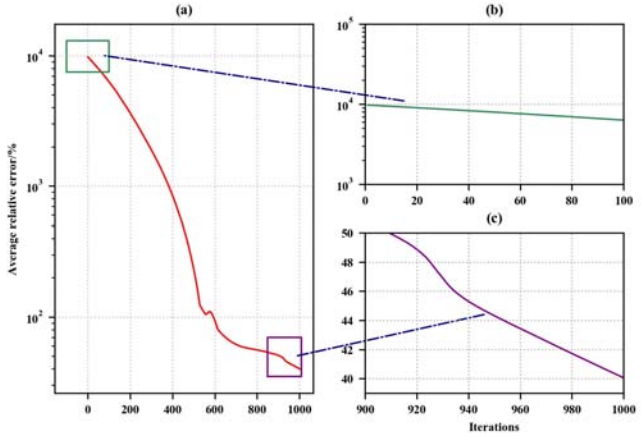

Figure 4. The variation of average relative error during 1000 training iterations: (a) The whole training process. (b) The first 100 iterations. (c) The last 100 iterations.

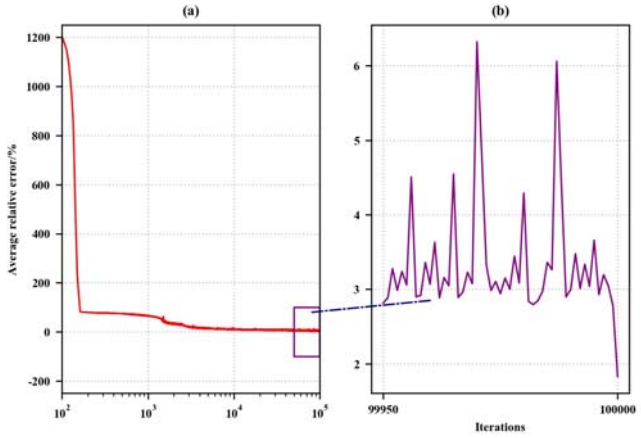

Figure 5. Curve of the average relative error corresponding to 100,000 iterations: (a) The whole training process. (b) The last 50 iterations.

In order to improve the training accuracy of BP neural network, the number of iterations is set to 100,000, and the average relative errors are shown in Fig. 5. When 100,000 training sessions are completed, the final average relative error is below 2%, which indicates that the training results are good. Then save the model after training as final model.

In addition, we need to select partial data as the validation set to examine the generalization ability and practical application ability of the model. For the battery 5#, the total number of charging and discharging cycles is 168, which can be roughly divided into three different capacity attenuation stages: early stage, medium stage and final stage. To verify the accuracy of model in each stage, the 38th, 88th and 152th discharging processes of battery 5# are randomly selected as the validation data in this study, as shown in Fig. 6.

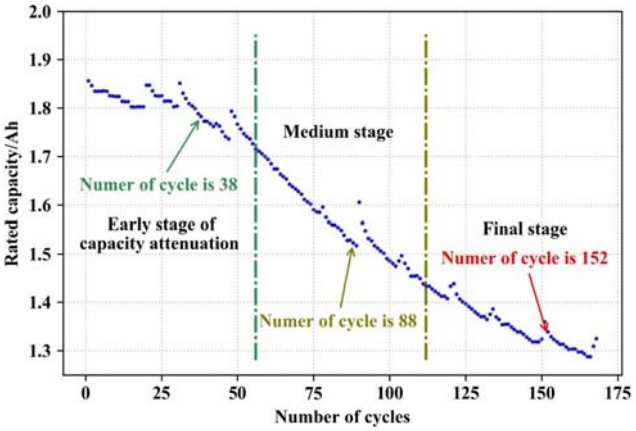

Figure 6. Validation data from three different stages of capacity attenuation.

The discharge current-time curves of 38th, 88th and 152th discharging processes are shown in Fig. 7. And the relationship between time and discharge current can be obtained by linear fitting:

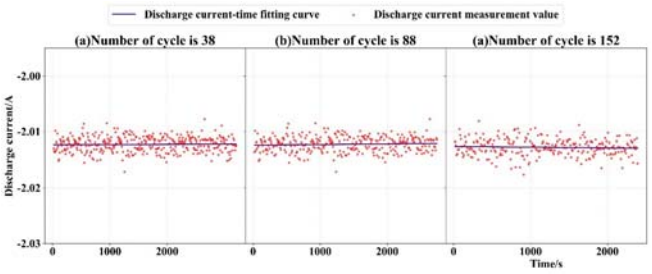

Figure 7. Discharge current-time fitting curves of the three discharging processes: (a) Number of cycle is 38. (b) Number of cycle is 88. (c) Number of cycle is 152.

Number of cycle is 38:

$$I = -2.01225 + 4.13507*10^{-8}*t \quad (14)$$

Number of cycle is 88:

$$I = -2.01291 + 1.73745*10^{-7}*t \quad (15)$$

Number of cycle is 152:

$$I = -2.01245 - 1.45337*10^{-7}*t \quad (16)$$

The calculated current rated capacity value of the battery and integrated value of the current with respect to time are substituted into the improved ampere-hour counting method, then the SOC of the three discharging processes are calculated separately, which is shown in Fig. 8 (a). And the BP neural network obtained after training is used to estimate the SOC variation during the three discharging processes, and the estimation results are shown in Fig. 8 (b).

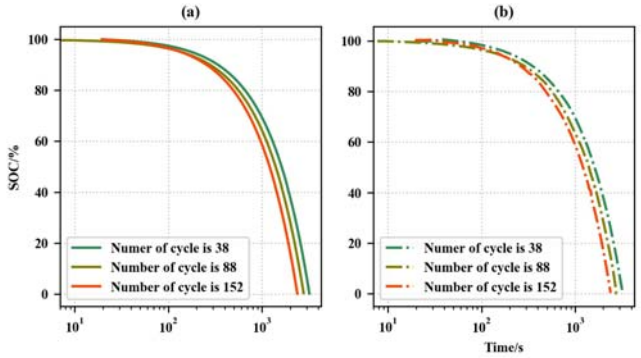

Figure 8. SOC estimation of 38th, 88th and 152th discharging process: (a) Using improved ampere-hour counting method. (b) Using BP neural network.

Moreover, average relative errors and absolute errors between the two SOC estimation of the 38th, 88th and 152th discharging process are also calculated separately, as shown in Fig. 9, Fig. 10 and Fig. 11.

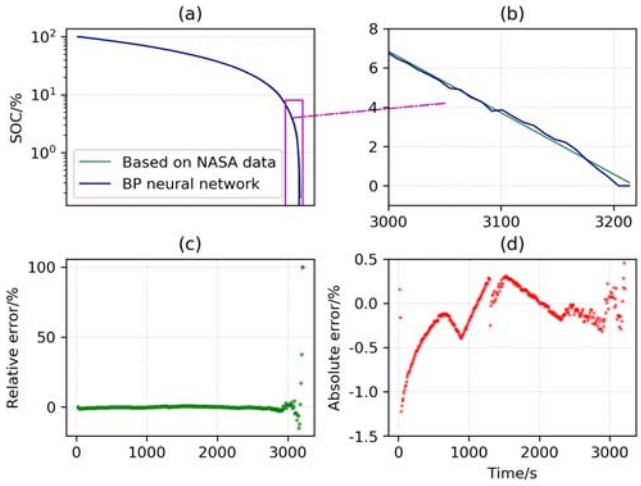

Figure 9. (a)(b) Comparison of SOC estimation results of the 38th discharging process. (c) Relative errors between two estimation results. (d) Absolute errors between two estimation results.

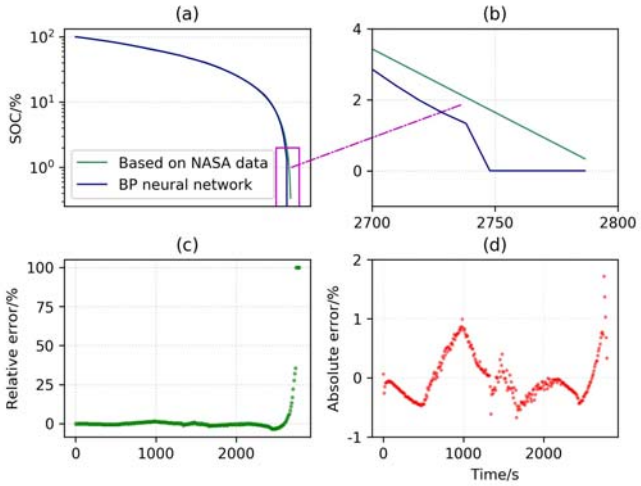

Figure 10. (a)(b) Comparison of SOC estimation results of the 88th discharging process. (c) Relative errors between two estimation results. (d) Absolute errors between two estimation results.

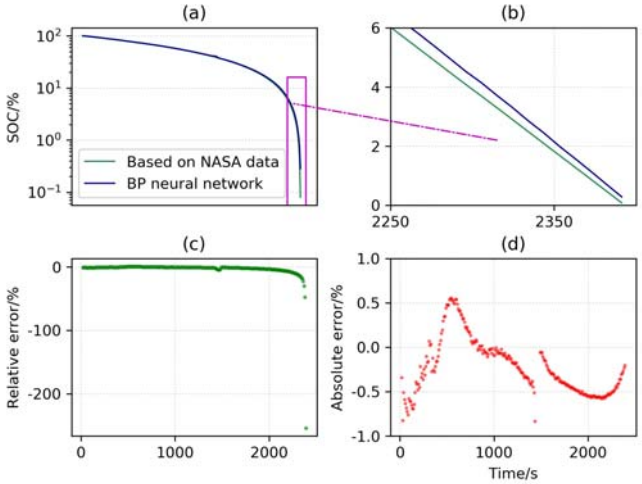

Figure 11. (a)(b) Comparison of SOC estimation results of the 152th discharging process. (c) Relative errors between two estimation results. (d) Absolute errors between two estimation results.

It can be seen from Fig. 9, Fig. 10 and Fig. 11 that the SOC estimation by BP neural network are highly consistent with the validation data. The average relative errors of the estimation results are 0.36%, 2.02% and 3.01%, respectively, and the maximum absolute errors are only 1.22%, 1.72% and 1.78%, respectively, which indicate that the BP neural network can accurately describe the nonlinear relationship between the SOC and the battery voltage, current, battery surface temperature, measurement time and number of cycles in the whole capacity attenuation process. It is worth noting that the relative errors have increased sharply when SOC of validation data is reduced to 5%, but the corresponding absolute errors are still at a low level. This is because that even a small SOC estimation deviation will also bring a large relative error when theoretical SOC is very small.

To further verify the feasibility of this method, lithium-ion battery with the rated capacity of 27Ah is used to carry out accelerated life experiment. The battery is charged with a constant current (CC) of 1C to the upper limit voltage of 4.20V, followed by a constant voltage (CV) at 4.20 V charging until it reaches C/10 to cut off the charging. After 30 minutes of rest, a CC of 3 C is applied to discharge the cells to the lower limited voltage at 2.75 V. The whole experiment is carried out in a thermotank at 40 degrees.

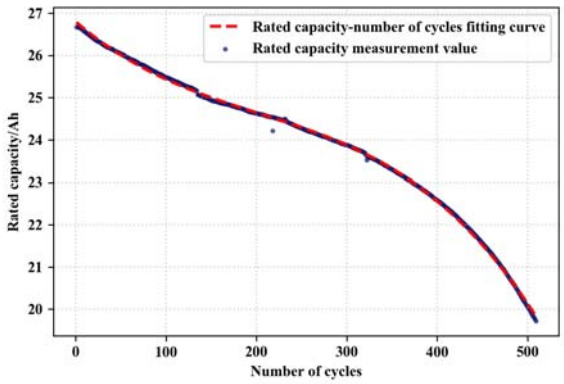

Figure 12. Rated capacity-number of cycles fitting curve using experiment data

The attenuation process of battery is shown in Fig. 12, which includes 509 cycles in total. Select input dataset, the number of hidden layer neurons, activation function and error function according to the methods described in Section 3, then establish new neural network, and the model is retained when training process finished. To validate the estimation accuracy of the model, 85th, 255th and 425th discharging processes are selected as validation data, which represent three different attenuation stages of battery. The validation results are shown in Fig. 13, Fig. 14 and Fig. 15.

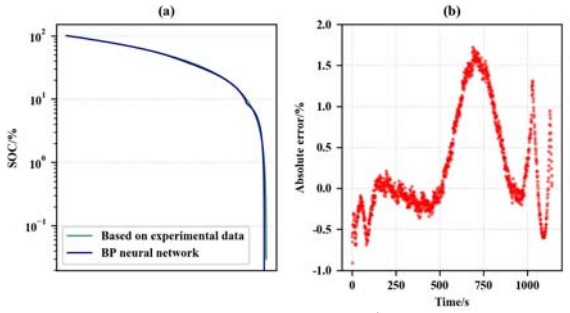

Figure 13. (a) SOC validation results of the 85th discharging process. (b) Absolute errors of SOC estimation results.

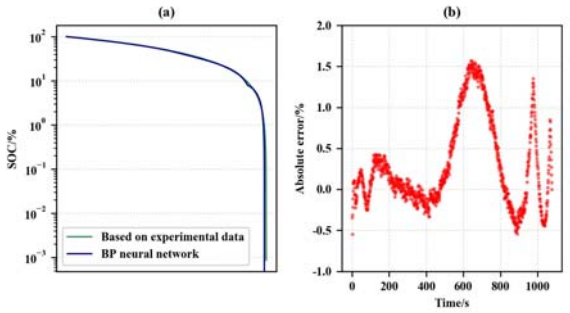

Figure 14. (a) SOC validation results of the 255th discharging process. (b) Absolute errors of SOC estimation results.

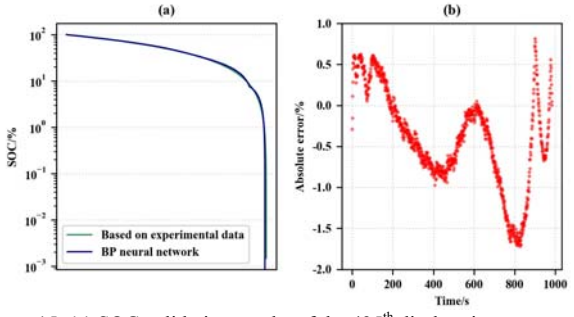

Figure 15. (a) SOC validation results of the 425th discharging process. (b) Absolute errors of SOC estimation results.

As we can see from validation results, the SOC curves estimated by BP neural network have high coincidence with experimental data, and the maximum absolute errors are only 1.72%, 1.57% and -1.72%, respectively. Hence, BP neural network with consideration of capacity attenuation can estimate SOC accurately during the battery life.

V. Conclusion

Accurate battery SOC estimation can contribute to reliable and safe battery utilization. In this paper, considering the impact of battery capacity attenuation on SOC estimation during the process of charging and discharging, an improved ampere-hour counting method is put forward so as to improve the precision of training data of BP neural network. At first, the theoretical SOC is calculated by the improved method based on NASA lithium-ion battery data. Next, BP neural network is constructed after the selection of each layer's nodes, activation function, error function, optimizer and learning rate. And the model after many training iterations is finally saved. Then the accuracy of model in each capacity attenuation stage is validated by three different discharging processes, and the results indicate that this proposed method can achieve desirable estimates even if the battery capacity continues to decline. Moreover, lithium-ion battery with the rated capacity of 27Ah is used to carry out accelerated life experiment to validate the feasibility of this method. The validation results show that the method has high accuracy and good applicability in estimating SOC. The main contributions of this work can be summarized as below.

(a) An improved ampere-hour counting method with consideration of capacity attenuation is proposed to calculate SOC, which enhances the accuracy of SOC calculation in different capacity attenuation stage.

(b) BP neural network is combined with improved ampere-hour counting method to estimate SOC. The maximum absolute errors of SOC estimation can be confined to an error band of ±2.0% at different aging cycles.

Acknowledgment

Project Supported by the National Key Research and Development Program of China (2016YFB0901900).

References

[1] O. Erdinc, B. Vural, M. Uzunoglu, "A dynamic lithium-ion battery model considering the effects of temperature and capacity fading," 2009 International Conference on Clean Electrical Power, Capri, 2009, pp. 383-386. doi: 10.1109/ICCEP.2009.5212025

[2] Languang Lu, Xuebing Han, Jianqiu Li, Jianfeng Hua, Minggao Ouyangl, "A review on the key issues for lithium-ion battery management in electric vehicles," Journal of Power Sources, vol. 226, pp. 272-288, Mar. 2013. doi: 10.1016/j.jpowsour.2012.10.060

[3] R. Dedryvère, et al, "Electrode/Electrolyte interface reactivity in high-voltage spinel $LiMn_{1.6}Ni_{0.4}O_4/Li_4Ti_5O_{12}$ lithium-ion battery," The Journal of Physical Chemistry C, vol. 114, pp. 10999-11008, May. 2010. doi: 10.1021/jp1026509

[4] Bin Wang, Jun Xu, Binggang Cao, Xuan Zhou, "A novel multimode hybrid energy storage system and its energy management strategy for electric vehicles," Journal of Power Sources, vol. 281, pp. 432-443, 1. May. 2015. doi: 10.1016/j.jpowsour.2015.02.012

[5] CHEN Y., MA Y., CHEN H., "State of charge and state of health estimation for lithium-ion battery through dual sliding mode observer based on amesim-simulink co-simulation," Journal of Renewable and Sustainable Energy, vol. 10, pp. 034103, Jun. 2018. doi: 10.1063/1.5012602

[6] Changfu Zou, Chris Manzie, Dragan N, Abhijit G.Kallapur, "Multi-Time-Scale observer design for state-of-charge and state-of-health of a lithium-ion battery," Journal of Power Sources, vol. 335, pp. 121-130, Dec. 2016. doi: 10.1016/j.jpowsour.2016.10.040

[7] D. O. Feder, M. J. Hlavac, "Analysis and interpretation of conductance measurements used to assess the state-of-health of valve regulated lead acid batteries," Proceedings of Intelec 94, International Telecommunications Energy Conference, Vancouver, 1994, pp. 282-291. doi: 10.1109/INTLEC.1994.396621

[8] He Y., Liu X., Zhang C., Chen Z., "A new model for State-of-Charge (SOC) estimation for high-power Li-ion batteries," Applied Energy, vol. 101, pp. 808-814, Jan. 2013. doi: 10.1016/j.apenergy.2012.08.031

[9] Pan H., Lü Z., Lin W., Li J., Chen L., "State of charge estimation of lithium-ion batteries using a grey extended Kalman filter and a novel open-circuit voltage model," Energy, vol. 138, pp. 764-75, Nov. 2017. doi: 10.1016/j.energy.2017.07.099

[10] Shi W., Hu X., Wang J., Jiang J., Zhang Y., Yip T., "Analysis of thermal aging paths for large-format $LiFePO_4$/graphite battery,"

Electrochimica Acta, vol. 196, pp. 13-23, Apr. 2016. doi: 10.1016/j.electacta.2016.02.161

[11] Yang Y., Hu X., Pei H., Peng Z., "Comparison of power-split and parallel hybrid powertrain architectures with a single electric machine: dynamic programming approach," Applied Energy, vol. 168, pp. 683-690, Apr. 2016. doi: 10.1016/j.apenergy.2016.02.023

[12] Chen L., Lin W., Li J., Tian B., Pan H., "Prediction of lithium-ion battery capacity with metabolic grey model," Energy, vol.106, pp. 662-672, Jul. 2016. doi: 10.1016/j.energy.2016.03.096

[13] Waag, Wladislaw, C. Fleischer, D. U. Sauer, "Critical review of the methods for monitoring of lithium-ion batteries in electric and hybrid vehicles," Journal of Power Sources, vol. 258, pp. 321-339, Jul. 2014. doi: 10.1016/j.jpowsour.2014.02.064

[14] J. H. Aylor, A. Thieme, B. W. Johnso, "A battery state-of-charge indicator for electric wheelchairs," IEEE Transactions on Industrial Electronics, vol. 39, pp. 398-409, Oct. 1992. doi: 10.1109/41.161471.

[15] Roscher MA, Sauer DU, "Dynamic electric behavior and open-circuit-voltage modeling of $LiFePO_4$-based lithium ion secondary batteries," Journal of Power Sources, vol. 196, pp. 331-336, Jan.2011. doi: 10.1016/j.jpowsour.2010.06.098

[16] Chiang Y.H., Sean W.Y., Ke J.C., "Online estimation of internal resistance and open-circuit voltage of lithium-ion batteries in electric vehicles," Journal of Power Sources, vol. 196, pp. 3921–3932, Apr. 2011. doi: 10.1016/j.jpowsour.2011.01.005

[17] Charkhgard M., Farrokhi M., "State-of-charge estimation for lithium-ion batteries using neural networks and EKF," IEEE Transactions on Industrial Electronics, vol. 57, pp. 4178–4187, Dec. 2010. doi: 10.1109/TIE.2010.2043035

[18] Miyamoto, Hiroyuki, M. Morimoto, K. Morita, "Online SOC estimation of battery for wireless tramcar," Electrical Engineering in Japan, vol. 186, pp. 83-89, Jan. 2014. doi: 10.1002/eej.21174

[19] Li Z., Huang J., Liaw B.Y., Zhang J., "On state-of-charge determination for lithium-ion batteries," Journal of Power Sources, vol. 348, pp. 281-301, Apr. 2017. doi: 10.1016/j.jpowsour.2017.03.001

[20] Piller, Sabine, M. Perrin, A. Jossen, "Methods for state-of-charge determination and their applications," Journal of Power Sources, vol. 96, pp. 113-120, Jun. 2001. doi: 10.1016/s0378-7753(01)00560-2

[21] Wei Z., Zhao J., Skyllas-Kazacos M., Xiong B., "Dynamic thermal-hydraulic modeling and stack flow pattern analysis for all-vanadium redox flow battery," Journal of Power Sources, vol. 260, pp. 89-99, Aug. 2014. doi: 10.1016/j.jpowsour.2014.02.108

[22] Wei Z., Zhao J., Xiong B., "Dynamic electro-thermal modeling of all-vanadium redox flow battery with forced cooling strategies," Applied Energy, vol. 135, pp. 1-10, Dec. 2014. doi: 10.1016/j.apenergy.2014.08.062

[23] Hu X., Li S., Peng H., "A comparative study of equivalent circuit models for Li-ion batteries," Journal of Power Sources, vol.198, pp. 359–367, Jan. 2012. doi: 10.1016/j.jpowsour.2011.10.013

[24] Meng J., Luo G., Gao F., "Lithium polymer battery state-of-charge estimation based on adaptive unscented Kalman Filter and support vector machine," IEEE Transactions on Power Electronics, vol. 31, pp. 2226–2238, Mar. 2016. doi: 10.1109/TPEL.2015.2439578

[25] Wang Y., Zhang C., Chen Z., "A method for state-of-charge estimation of Li-ion batteries based on multi-model switching strategy," Applied Energy, vol. 137, pp. 427–434, Jan. 2015. doi: 10.1016/j.apenergy.2014.10.034

[26] Pérez G., Garmendia M., Reynaud J.F., Crego J., Viscarret U., "Enhanced closed loop state of charge estimator for lithium-ion batteries based on Extended Kalman Filter," Applied Energy, vol. 155, pp. 834–845, Oct. 2015. doi: 10.1016/j.apenergy.2015.06.063

[27] He H., Xiong R., Peng J., "Real-time estimation of battery state-of-charge with unscented Kalman filter and RTOS μCOS-II platform," Applied Energy, vol. 162, pp. 1410–1418, Jan. 2016. doi: 10.1016/j.apenergy.2015.01.120

[28] Lim K., Bastawrous H.A., Duong V.-H., See K.W., Zhang P., Dou S.X., "Fading Kalman filter-based real-time state of charge estimation in $LiFePO_4$ battery-powered electric vehicles," Applied Energy, vol. 169, pp. 40–48, May. 2016. doi: 10.1016/j.apenergy.2016.01.096

[29] Wang Y, Zhang C, Chen Z, "A method for state-of-charge estimation of $LiFePO_4$ batteries at dynamic currents and temperatures using particle filter," Journal of Power Sources, vol. 279, pp. 306-311, Apr. 2015. doi: 10.1016/j.jpowsour.2015.01.005

[30] Wang Y., Zhang C., Chen Z., "A method for joint estimation of state-of-charge and available energy of $LiFePO_4$ batteries," Applied Energy, vol. 135, pp. 81-87, Dec. 2014. doi: 10.1016/j.apenergy.2014.08.081

[31] Lin C., Mu H., Xiong R., Shen W., "A novel multi-model probability battery state of charge estimation approach for electric vehicles using H-infinity algorithm," Applied Energy, vol.166, pp. 76-83, Mar. 2016. doi: 10.1016/j.apenergy.2016.01.010

[32] Chen X., Shen W., Cao Z., Kapoor A., "A novel approach for state of charge estimation based on adaptive switching gain sliding mode observer in electric vehicles," Journal of Power Sources, vol. 246, pp. 667-678, Jan. 2014. doi: 10.1016/j.jpowsour.2013.08.039

[33] Du J., Liu Z., Wang Y., Wen C., "An adaptive sliding mode observer for lithium-ion battery state of charge and state of health estimation in electric vehicles," Control Engineering Practice, vol. 54, pp. 81-90, Sep. 2016. doi: 10.1016/j.conengprac.2016.05.014

[34] G.L. Plett, "Extended Kalman filtering for battery management systems of LiPB-based HEV battery packs: Part 3. state parameter estimation," Journal of Power Sources, vol. 134, pp. 277–292, Aug. 2004. doi: 10.1016/j.jpowsour.2004.02.033

[35] Chiang Y.H., Sean W.Y., Ke J.C., "Online estimation of internal resistance and open-circuit voltage of lithium-ion batteries in electric vehicles," Journal of Power Sources, vol. 196. pp. 3921–3932, Apr. 2011. doi: 10.1016/j.jpowsour.2011.01.005

[36] Charkhgard M., Farrokhi M., "State-of-charge estimation for lithium-ion batteries using neural networks and EKF," IEEE Transactions on Industrial Electronics, vol. 57, pp. 4178–4187, Feb. 2010. doi: 10.1109/TIE.2010.2043035

[37] Deng Z., Yang L., Cai Y., Deng H., Sun L., "Online available capacity prediction and state of charge estimation based on advanced data-driven algorithms for lithium iron phosphate battery," Energy, vol. 112, pp. 469-480, Oct. 2016. doi: 10.1016/j.energy.2016.06.130

[38] Alvin J. Salkind, Craig Fennie, Pritpal Singh, Terrill Atwater, David E Reisner "Determination of state-of-charge and state-of-health of batteries by fuzzy logic methodology," Journal of Power Sources, vol. 80, pp. 293-300, Jul. 1999. doi: 10.1016/s0378-7753(99)00079-8

[39] Malkhandi S., "Fuzzy logic-based learning system and estimation of state-of-charge of lead-acid battery," Engineering Application of Artificial Intelligence, vol. 19, pp. 479-485, Aug. 2006. doi: 10.1016/j.engappai.2005.12.005

[40] Sheng H., Xiao J., "Electric vehicle state of charge estimation: nonlinear correlation and fuzzy support vector machine," Journal of Power Sources, vol. 281, pp. 131-137, May. 2015. doi: 10.1016/j.jpowsour.2015.01.145

[41] Hussein A.A., "Derivation and comparison of open-loop and closed-loop neural network battery state-of-charge estimators," 7th International Conference on Applied Energy (ICAE), Abu Dhabi, 2015, pp. 1856-1861. doi: 10.1016/j.egypro.2015.07.163.

[42] Zou Y., Hu X., Ma H., Li S.E., "Combined state of charge and state of health estimation over lithium-ion battery cell cycle lifespan for electric vehicles," Journal of Power Sources, vol. 273, pp. 793-803, Jan. 2015. doi: 10.1016/j.jpowsour.2014.09.146

[43] Haihong Pan, Zhiqiang Lü, Weilong Li, Junzi Li, LinChen, "State of charge estimation of lithium-ion batteries using a grey extended Kalman filter and a novel open-circuit voltage model," Energy, vol. 138, pp. 764-775, Nov. 2017. doi: 10.1016/j.energy.2017.07.099

[44] N. Watrin, B. Blunier, A. Miraoui, "Review of adaptive systems for lithium batteries state-of-charge and state-of-health estimation," 2012 IEEE Transportation Electrification Conference and Expo (ITEC), Dearborn, 2009, pp. 1-6. doi: 10.1109/ITEC.2012.6243437

[45] Xiong R., Gong X., Mi C.C., Sun F., "A robust state-of-charge estimator for multiple types of lithium-ion batteries using adaptive extended Kalman filter," Journal of Power Sources, vol. 64, pp. 805-816, Dec. 2013. doi: 10.1016/j.jpowsour.2013.06.076

[46] Ramadesigan V., Chen K., Burns N. A., et al, "Parameter estimation and capacity fade analysis of lithium-ion batteries using reformulated models," Journal of the Electrochemical Society, vol. 158, pp. A1048-A1054, Jul. 2011. doi: 10.1149/1.3609926

[47] Hu X., Li S.E., Jia Z., Egardt B., "Enhanced sample entropy-based health management of Li-ion battery for electrified vehicles," Energy, vol. 64, pp. 953-960, Jan. 2014. doi: 10.1016/j.energy.2013.11.061

[48] Hu C., Youn B.D., Chung J., "A multiscale framework with extended Kalman filter for lithium-ion battery SOC and capacity estimation," Applied Energy, vol. 92, pp. 694-704, Apr. 2012. doi: 10.1016/j.apenergy.2011.08.002

[49] Wei He, Nicholas Williard, Chaochao Chen, Michael Pecht, "State of charge estimation for Li-Ion batteries using neural network modeling and unscented Kalman filter-based error cancellation," International Journal of Electrical Power & Energy Systems, vol. 62, pp. 783-791, Nov. 2014. doi: 10.1016/j.ijepes.2014.04.059

[50] He W., Williard, N., Chen, C. C., Pecht M., "State of charge estimation for Li-ion batteries using neural network modeling and unscented Kalman filter-based error cancellation," International Journal of Electrical Power & Energy Systems, vol. 62, pp. 783–791, Nov. 2014. doi: 10.1016/j.ijepes.2014.04.059